Polarization and Internal Electric Field in Aromatic Polyamides Based on *m*-Xylylenediamine with Linear Aliphatic Dicarboxylic Acids

Naoto Tsutsumi,* Toshio Iyo, Wataru Sakai, and Tsuyoshi Kiyotsukuri

Department of Polymer Science & Engineering, Kyoto Institute of Technology, Matsugasaki, Sakyo, Kyoto 606, Japan

Received March 12, 1996; Revised Manuscript Received August 26, 1996[⊗]

ABSTRACT: Polarization reversal and internal electric field were studied for the aromatic polyamides of *m*-xylylenediamine (MXD) with linear aliphatic dicarboxylic acids in which the number of methylene groups is in the range of 4−10. Polarization reversal was measured for all MXD polyamides at room temperature and at a temperature just above the glass transition temperature (T_g). Large polarization was measured for the polyamides with odd numbers of methylene groups in a dicarboxylic acid unit poled at temperatures above T_g. Internal electric field was measured from the electrochromic spectrum shift and broadening of the probe molecule of 4-(dimethylamino)-4′-nitrostilbene in the polyamides with even numbers of methylene groups in a dicarboxylic acid unit. Large internal electric field was measured for the samples in which the remanent polarization measured from the polarization reversal is small. The large internal electric field is mainly ascribed to the space charges created by the injected charges. Upon thermal annealing, the small depression of the internal electric field was measured in the vicinity of T_g, but it is stable until its significant depression occurs around the cold crystallization temperature of polyamides. Thermally stimulated discharge current profiles gave the broad peaks in the same temperature regions where the large depression of internal electric field occurred. These results imply the release of injected charges from the sample film.

Introduction

Ferroelectricity of polymers has been investigated for the vinylidene fluoride polymers since the 1980s. Polarization reversals of poly(vinylidene fluoride) (PVDF)[1] and copolymers of vinylidene fluoride and trifluoroethylene (P(VDF-TrFE))[2] were shown to have originated from the cooperative switching of β crystallite dipoles. A clear Curie transition temperature was measured in P(VDF-TrFE).[2] The ferroelectric properties of the aliphatic polyamide of nylon 11 and 7[3−6] and the aromatic polyamide[7] have also been studied.

We have studied the internal electric field created by the aligned β crystallite dipoles for P(VDF-TrFE),[8] the blend of PVDF and poly(methyl methacrylate) (PMMA),[9] and the P(VDF-TrFE)/PMMA blend.[10] Internal electric field is measured using the electrochromic spectrum change of probe molecules dispersed in the matrix. Internal electric field is on the order of megavolts per centimeter depending on the achieved polarization, which is a few times larger than the poling field.

In this study, polarization and internal electric field are studied for the aromatic polyamides of *m*-xylylenediamine with linear aliphatic dicarboxylic acids in which the number of methylene groups is in the range of 4−10. Polarization reversal is discussed in terms of the alignment of the amorphous dipole moments, and internal electric field is discussed in terms of the effects of the space charges created by countercharges accumulated near amorphous amide dipoles.

Experimental Section

Preparation of Aromatic Polyamides. Aromatic polyamides of *m*-xylylenediamine (MXD) and linear aliphatic dicarboxylic acids (*n*) with methylene numbers from 4 to 10 were prepared. Linear aliphatic dicarboxylic acids are adipic (n = 6), pimelic (7), suberic (8), azelaic (9), sebacic (10), and dodecanedioic (12) acids. Obtained polyamides are named as MXD*n*; for example, MXD6 is the polyamide of MXD with adipic acid (n = 6).

MXD*n* salt was prepared from MXD and *n* in ethyl alcohol at 70 °C for 4 h. After filtration and subsequent drying, MXD*n* salt was polymerized at 200−260 °C for 1 h at atmospheric pressure and for 2 h under a reduced pressure of 0.2−1.0 Torr. Polymerization temperatures of MXD6 and MXD7 are 260 and 240 °C, respectively, those of MXD8 and MXD9 are 220 °C, and those of MXD10 and MXD12 are 210 and 200 °C, respectively. These polymerization temperatures are 10−20 °C higher than the corresponding melting temperatures.

Sample Film Preparation. Obtained polyamides were melt-pressed between Teflon-coated polyimide films or aluminum plates on a heated press. The molten films were quenched into liquid nitrogen. Aluminum plates were dissolved in 10 wt % sodium hydroxide solution. 4-(Dimethylamino)-4′-nitrostilbene (DANS) molecules were introduced by soaking the polyamide films in 1-propyl alcohol solution saturated with DANS dye in the vicinity of the glass transition temperature (T_g) of each polyamide for 2 h, followed by drying for 6 h at 80 °C in vacuo. The films with DANS melted in a heated press were then quenched again into liquid nitrogen.

Poling. Several cycles of 0.05 Hz sinusoidal voltage or a constant voltage were applied for 1 h to the aluminum electrodes, which had been evaporated onto opposing surfaces of the films in a 3 M inert liquid Fluorinert FC40, which was held at room temperature or at a temperature just above T_g: 80 °C for MXD6, 70 °C for MXD7, 60 °C for MXD9, 55 °C for MXD10, and 45 °C for MXD12. In the case of poling at temperatures above T_g, the first 30 min is for the poling process above T_g, and the following 30 min is for the cooling down process while cyclic high voltage is applied.

Electrical and Optical Measurements. The pyroelectric coefficient (C_{pyro}) was determined by measuring the current generated upon heating and cooling the poled film at a measured rate of 1−2 °C/min in the vicinity of 30 °C. Thermally stimulated discharge current (TSC) was measured by the current flow in the external circuit under a constant temperature increase rate of 4 °C/min, using the sandwich-type cell with the poled surface grounded. Ultraviolet−visible spectra of the films were measured in transmission on a UV−

[⊗] Abstract published in *Advance ACS Abstracts,* November 15, 1996.

S0024-9297(96)00374-9 CCC: $12.00

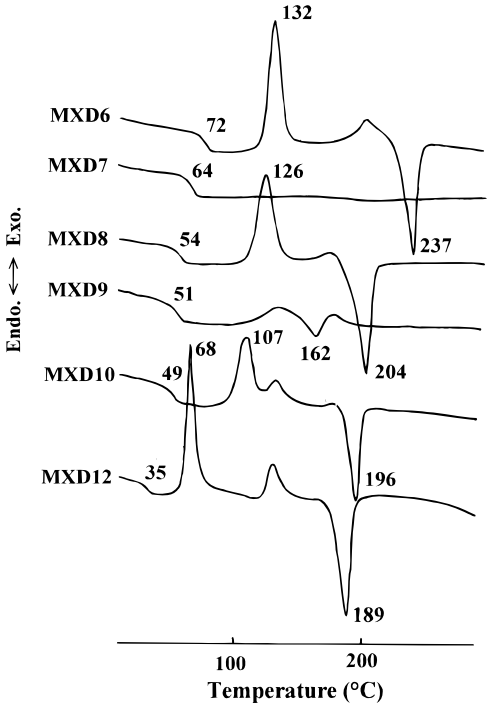

Figure 1. DTA thermograms of melt-quenched films.

visible spectrometer after the aluminum electrodes were removed by immersing them in 10 wt % sodium hydroxide solution for a few minutes.

Characterization. Differential thermal analysis (DTA) was carried out at a heating rate of 10 °C/min in a nitrogen atmosphere on a differential thermal analyzer. Wide-angle X-ray scattering (WAXS) patterns of the films were measured on a X-ray diffractometer with nickel-filtered Cu Kα radiation.

Results and Discussion

Polymer Structure. Figure 1 shows DTA thermograms of melt-quenched sample films. All polyamide films have a clear heat capacity change due to the glass transition. T_g values decrease with increasing the number of methylene groups, which is ascribed to the increase of the total number of flexible methylene groups in the molar unit. Thermograms for polyamides from the even number dicarboxylic acids give clear exothermic peaks (T_{cc}) due to cold crystallization, followed by endothermic peaks (T_m) due to crystallite melting. However, the thermogram of MXD7 only gives the heat capacity change due to T_g, and that of MXD9 has a small and broad endothermic melting peak in addition to the heat capacity change due to the glass transition. Figure 2 shows the WAXS patterns of the films melt-quenched and subsequently annealed for 1.5 h at 80 °C for MXD6 and at 70 °C for MXD7. The WAXS pattern of the annealed MXD6 film shows the crystallite diffraction pattern in addition to the amorphous halo, but that of the annealed MXD7 only gives the amorphous halo. These DTA thermogram and WAXS pattern results show that the polyamides with even numbers of dicarboxylic acid units easily crystallize at temperatures above T_g.

Polarization Current and Polarization Charge. Figure 3 shows the polarization current and its time integral (polarization charge) for MXD9 as a function of sinusoidal applied electric field with a maximum field of 0.8 MV/cm at a temperature above T_g. Current flow in the external circuit is the summation of the current

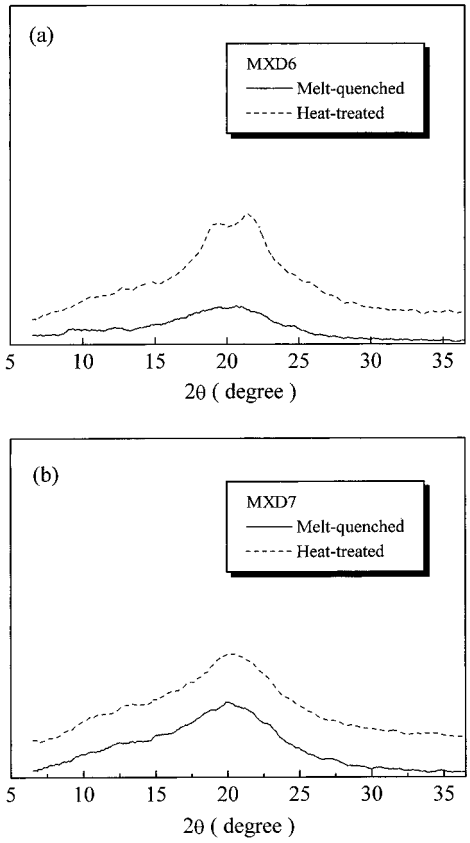

Figure 2. WAXS patterns of melt-quenched and thermally annealed films (a) at 80 °C for MXD6 and (b) at 70 °C for MXD7.

due to the polarization, capacitance, and conductivity,[11] i.e.,

$$J = J_D + J_\rho = \frac{dP}{dt} + \epsilon\epsilon_0\frac{dE_p}{dt} + \frac{E}{\rho} \qquad (1)$$

where J is the poling current with unit of A/cm^2, J_D is the displacement current, J_ρ is the conduction current, ϵ is the relative permittivity, ϵ_0 is the permittivity of a vacuum, P is polarization, E_p is applied electric field, and ρ is resistivity. The polarization current in Figure 3 is the poling current reduced by the terms of capacitance and conductivity. In the polarization charge profile in Figure 3b, the remanent polarization (P_r) is the value of polarization at zero applied field, and the cohesive field (E_c) is the applied field at zero polarization after the last cycle of poling. E_c values were in the range of 0.45−0.55 MV/cm.

Figure 4 shows the dependence of C_{pyro} on the poling field for MXD6 and -7. For both cases, C_{pyro} largely increases at the poling field above 0.3−0.4 MV/cm, which is close to E_c values, and reaches 1.5 nC/(cm^2 K) at the poling field of 0.8 MV/cm. Figure 5 shows the dependence of P_r on applied electric field when MXD6, -7, -9, -10, and -12 films are sinusoidally poled at room temperature (open symbols) and at temperatures above T_g (closed symbols). P_r values increase with increasing E_p at applied electric fields above E_c. P_r values for MXD7 and -9 obtained at temperatures above T_g and at higher field above E_c are much higher than those obtained at room temperature and at the same field, whereas for MXD6, -10, and -12 there is no significant difference in E_p-P_r profiles between room temperature poling and poling above T_g. Namely, MXD7 and -9 have significantly different E_p-P_r profiles for the two poling

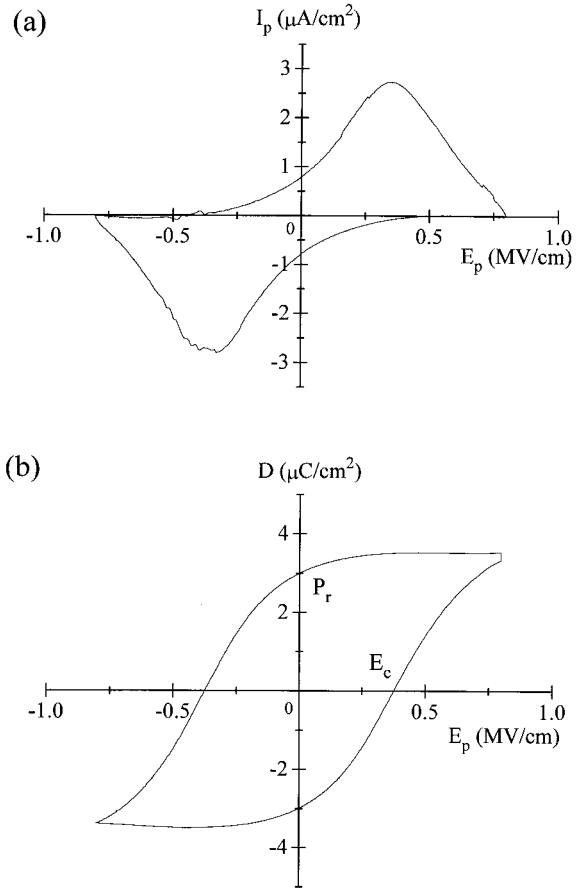

Figure 3. Polarization current (a) and polarization charge (time integral of polarization current, b) for MXD9 film poled at 0.8 MV/cm for 1 h at a temperature above T_g, 60 °C.

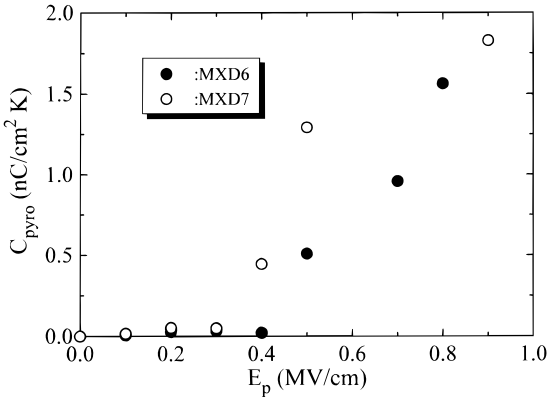

Figure 4. Dependence of C_{pyro} on E_p. Poling is carried out for 1 h at room temperature.

temperatures, but E_p-P_r profiles for MXD6, -10, and -12 are the same, irrespective of poling temperature. In a previous study reported by Murata et al.[7] for the polarization reversal of MXD*n* polyamides with n = 6−11 and 13, melt-quenched samples exhibited a D−E hysteresis loop, with a large P_r of 2.3−6.7 μC/cm^2, regardless of the number of carbon atoms in the acid unit. These large P_r values were achieved at a higher electric field of 2 MV/cm. It was pointed out that the possible origin of the ferroelectricity (polarization reversal) is likely related to the amorphous regions in these polyamides.[7] Large P_r values for the present MXD7 and -9 obtained from the polarization reversal at temperatures above T_g are ascribed to the alignment of the amorphous amide dipole moments assisted by the segmental molecular motion above T_g. Because only the

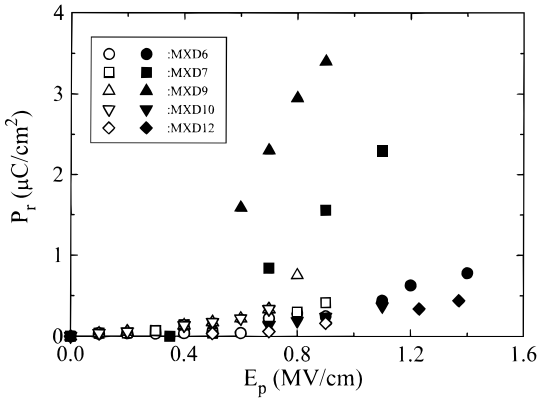

Figure 5. Dependence of P_r on E_p. Open symbols: Poled at room temperature. Closed symbols: Poled at temperatures above T_g (80 °C for MXD6; 70 °C for MXD7; 60 °C for MXD9; 55 °C for MXD10; and 45 °C for MXD12).

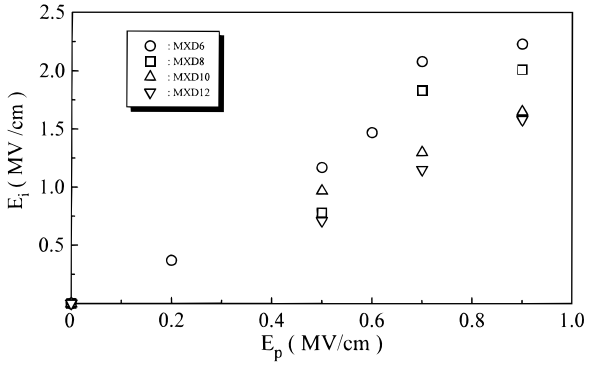

Figure 6. Dependence of E_i on E_p. Poling condition is the same as in Figure 4.

restricted local molecular motion is allowed in the matrix at room temperature, the smaller P_r values are obtained for all MXD*n* polyamides. The question arises as to why MXD6, -10, and -12 cannot achieve the large polarization even when poled at temperatures above T_g. As shown in Figures 1 and 2, MXD6, -10, and -12 easily crystallize at temperatures above T_g. A smaller P_r value for crystallized MXD6 was reported by Murata et al.[7] If the ferroelectricity of MXD*n* polyamides is related to the crystalline region, then the small values of P_r for crystallized MXD6 may be due to the compact packing of the hydrogen-bonded sheet,[7] as in the case of nylons 7 and 11.[6] Therefore, in the present case, the crystallization induced for MXD6, -10 and -12 when poled above T_g may be responsible for the smaller P_r values.

Internal Electric Field and Remanent Polarization for MXD6, -8, -10, and -12. Internal electric field (E_i) was measured by the spectrum shift and broadening of the probe molecule of DANS dispersed in the polyamide matrix, using the electrochromic theory.[12,13] As we did before, the difference between the absorption spectra before and after poling can be expressed as a Taylor series expansion with first, second, and higher orders of the derivatives of the unperturbed spectrum (spectrum before poling). The detailed derivation and calculation are expressed in our previous literature.[8,10]

Figure 6 shows the dependence of E_i on poling field for MXD6, -8, -10, and -12. In the preparation process, introducing DANS into MXD7 and -9 films, the films became too opaque for the UV−visible spectrum of DANS to be measured in these samples. Poling was carried out for 1 h at room temperature. E_i linearly increases with increasing E_p and reaches 1.5−2.5 MV/cm. Figure 7 shows the plots of P_r vs E_i. The increase

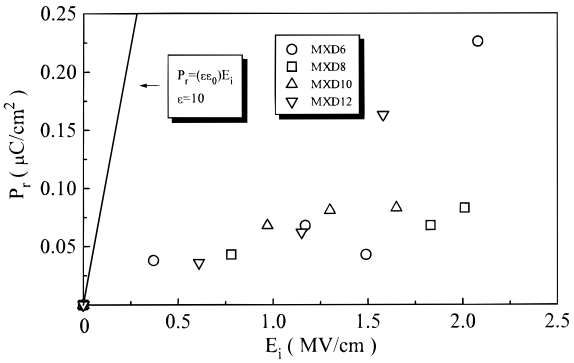

Figure 7. Plots of E_i vs P_r. The line is drawn using the equation $P_r = (10\epsilon_0)E_i$.

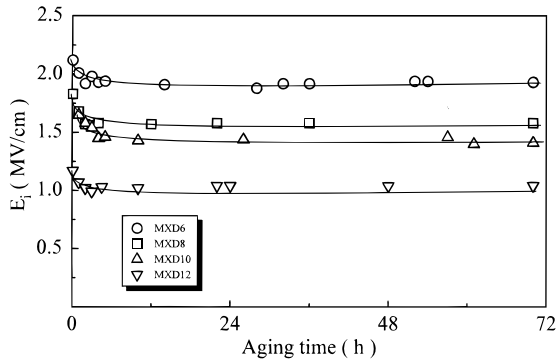

Figure 8. Dependence of E_i on aging time. Poling is carried out at 0.7 MV/cm for 1 h at room temperature.

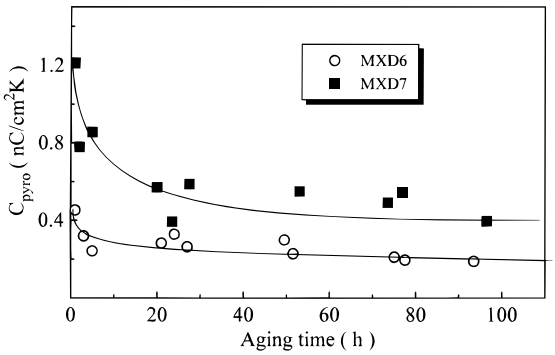

Figure 9. Dependence of C_{pyro} on aging time. Poling condition is the same as in Figure 8.

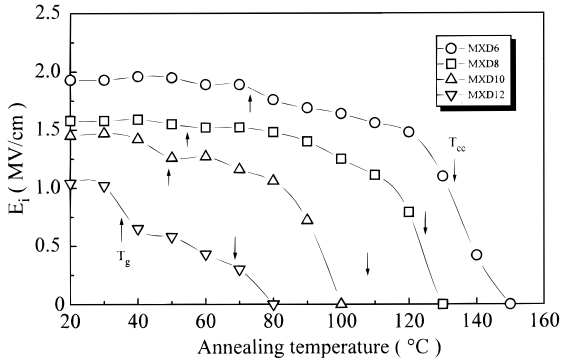

Figure 10. Temporal thermal stability of E_i upon heating. Up and down arrows in the figure indicate T_g and T_{cc} measured by a thermal analysis, respectively.

of E_i leads to the increase of P_r, but the P_r values are considerably smaller in contrast to the relatively larger E_i values. In the figure, the solid line shows the theoretical plot of $P_r = (\epsilon\epsilon_0)E_i$, where ϵ is the relative permittivity of polyamide and ϵ_0 is the permittivity of a vacuum.[8,14] The value of ϵ (= 10) was obtained from analysis of the polarization current. The obtained P_r values are much smaller than the expected values from the theoretical expression at a given E_i. Why can larger E_i be obtained irrespective of smaller P_r values? A possible explanation for the larger E_i is given by the effects of space charges injected from the electrodes, as in the case of the PVDF/PMMA blend.[9]

Thermal Stability of Internal Electric Field and TSC Results for MXD6, -8, -10, and -12. Figure 8 shows the plots of E_i after poling as a function of storage (aging) time at room temperature for MXD6, -8, -10, and -12. Poling was performed at a constant voltage of 0.7 MV/cm for 1 h at room temperature for all samples. Apart from the small depression of E_i during a few hours immediately following poling, E_i remains stable over the time interval of several days, which is in contrast to the fact that C_{pyro} largely decays for a few decade hours and still slowly relaxes after a few days after poling, as shown in Figure 9. As shown in Figure 8, E_i values have a clear dependence of the number of methylene groups, i.e., the concentration of amide group in the repeated molecular unit. This clear dependence of E_i on the amide group concentration implies that the injected charges reside near the polar amorphous amide dipoles and create the local space charges around them; thus, the space charge density is proportional to the concentration of amide groups in the repeated molar unit.

Figure 10 shows the dependence of E_i on the annealing temperature for the same samples shown in Figure 8. Annealing temperature profiles of E_i give the small depression of E_i in the vicinity of T_g, which is shown as an up arrow in the figure, and its subsequent stability until the large depression of E_i occurs around 135 °C for MXD6, 125 °C for MXD8, 95 °C for MXD10, and 70 °C for MXD12. These results are in contrast to the fact that the pyroelectric activity was largely depressed in the vicinity of T_g. These temperatures correspond well to the cold crystallization temperatures for each system, shown as a down arrow in the figure. This coincidence implies that the countercharges, which are responsible for the space charges, are excluded from the region near amorphous amide dipoles in which the ordered crystallite is growing and released from the matrix. The same type of dependence of the internal electric field on the annealing temperature was measured in the polymer blend system of PVDF and PMMA.[9] For PVDF/PMMA, the space charges due to the injected charges are considered to stabilize the internal electric field.[9]

Figure 11 shows the TSC profiles of MXD8 (a) and -12 (b) films poled at 0.7 MV/cm for 1 h at room temperature. A broad but clear peak appears in the vicinity of 100 °C for MXD8 and 60 °C for MXD12 in the first TSC run, and these peaks entirely disappear in the second TSC run for the same sample films that were already exposed in the first TSC heating. The temperature regions where these broad peaks appear correspond well to those where E_i values are significantly depressed, which are shown in Figure 10. Thus, the broad peaks in the TSC profiles are explained on the basis of the release of the injected charges from the sample films, i.e., the disappearance of the space charges in the sample.

Conclusion

The polarization and the internal electric field are investigated for the aromatic polyamide of MXD*n*, in which *n* is the number of aliphatic dicarboxylic acid

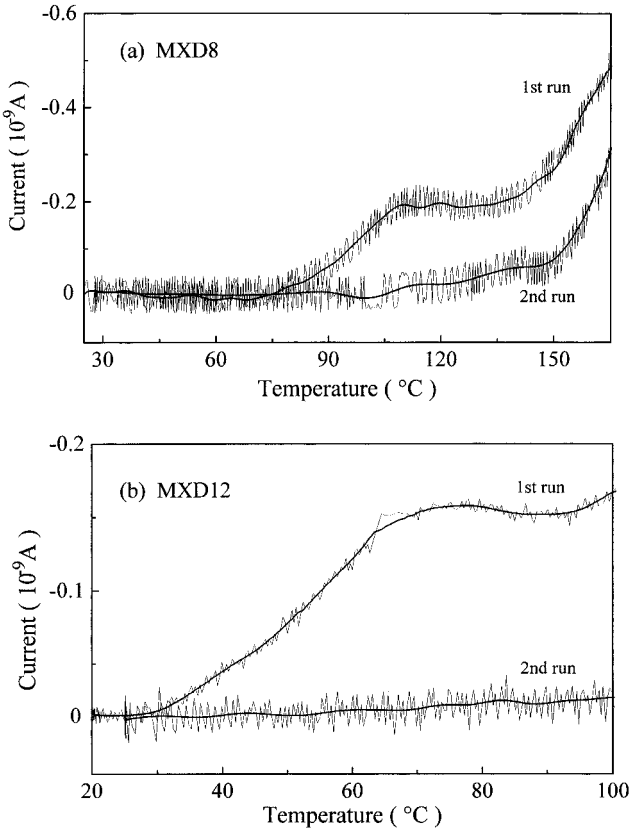

Figure 11. TSC profiles for MXD8 (a) and for MXD12 (b). Poling condition is the same as in Figure 8.

units with various methylene numbers. The polarization reversal was measured for all MXD polyamides at room temperature and at temperatures just above T_g. Large polarization was measured for MXD7 and -9 poled at temperatures above T_g, in which the significance of switching the amorphous dipole moments must be considered. The large internal electric field determined by the spectrum shift and broadening of the electrochromic probes of DANS were measured for MXD6, -8, -10, and -12, in which the remanent polarization measured from the polarization reversal is small. The space charges due to injected charges are responsible for the large internal electric field. Upon thermal annealing, a small depression of the internal electric field was measured in the vicinity of T_g, but it is stable until its significant depression is observed around the temperature near the cold crystallization temperature, in which the exclusion of charges near the amorphous amide dipoles occurs when the ordered crystallite is growing. Thermally stimulated discharge current profiles give broad peaks in the same temperature regions where the large depression of internal electric field occurs. These results imply the release of injected charges from the sample film.

References and Notes

(1) Furukawa, T.; Date, M.; Fukada, E. *J. Appl. Phys.* **1980**, *51*, 1135.
(2) Furukawa, T.; Lovinger, A. J.; Davis, G. T.; Broadhurst, M. G. *Macromolecules* **1983**, *16*, 1885.
(3) Newman, B. A.; Chen, P.; Pae, K. D.; Scheinbeim, J. I. *J. Appl. Phys.* **1980**, *51*, 5161.
(4) Mathur, S. C.; Scheinbeim, J. I.; Newman, B. A. *J. Appl. Phys.* **1984**, *56*, 2419.
(5) Lee, J. W.; Takase, Y.; Newman, B. A.; Scheinbeim, J. I. *J. Polym. Sci. Part B, Polym. Phys.* **1991**, *29*, 273.
(6) Lee, J. W.; Takase, Y.; Newman, B. A.; Scheinbeim, J. I. *J. Polym. Sci. Part B, Polym. Phys.* **1991**, *29*, 279.
(7) Murata, Y.; Tsunashima, K.; Koizumi, N.; Ogami, K.; Hosokawa, F.; Yokoyama, K. *Jpn. J. Appl. Phys.* **1993**, *32*, L849.
(8) Tsutsumi, N.; Davis, G. T.; DeReggi, A. S. *Macromolecules* **1991**, *24*, 6392.
(9) Tsutsumi, N.; Ueda, Y.; Kiyotsukuri, T.; DeReggi, A. S.; Davis, G. T. *J. Appl. Phys.* **1993**, *74*, 3366.
(10) Tsutsumi, N.; Ono, T.; Kiyotsukuri, T. *Macromolecules* **1993**, *26*, 5447.
(11) Bur, A. J.; Roth, S. C. *Preparation of Thin Film Polyvinylidene Fluoride Shock Wave Pressure Transducers*; Interagency Report 87-3680, NTIS PB881560070; U.S. National Bureau of Standards: Washington, DC, 1987.
(12) Liptay, W. In *Exited States*; Lim, E. C., Ed.; Academic Press: New York and London, 1974; Vol. I, pp 129−229.
(13) Havinga, E. E.; van Pelt, P. *Ber. Bunsen-Ges. Phys. Chem.* **1979**, *83*, 816.
(14) Sears. F. W. *Electricity and Magnetism*; Addison-Wesley Press: Cambridge, MA, 1951; pp 176−178.

MA9603746